

Shower measurements in the calorimeter for ILC

J. Cvach

*Institute of Physics of the ASCR, v. v. i., Praha
On behalf of the CALICE Collaboration*

I Introduction

The CALICE (CALorimetry for the LInear Collider Experiments) collaboration [1] is studying several designs of calorimeters [2] for experiments at the future International Linear Collider (ILC). In the first phase, characterised by the construction of “physics prototypes”, the feasibility of building a pixelised calorimeter is studied. The second phase, “technological prototypes” will focus on the engineering details needed to insert such a calorimeter in an ILC detector. In both phases, the prototypes will be subject to extensive studies at beam test facilities.

Physics at the ILC places stringent requirements on the detector, including the ability to measure jet energies with a precision of at least $0.3/\sqrt{(E_{jj}/\text{GeV})}$. It has been demonstrated in Monte Carlo (MC) simulations [3] that the Particle Flow Algorithm (PFA) [4] approach to the reconstruction of jet energies in terms of the individual particles can achieve this goal for typical jets at the ILC energies 500–1000 GeV in the centre-of-mass system.

Three highly granular physics prototype calorimeters constructed by the CALICE collaboration have been tested at the CERN beam during 2006 and 2007. The Silicon-Tungsten Electromagnetic Calorimeter (ECAL, [5]) with $1\times 1\text{ cm}^2$ readout pads; the scintillator-steel hadron calorimeter (AHCAL, [6]) with $3\times 3\text{ cm}^2$ tiles analogically readout; and the scintillator-steel Tail-Catcher and Muon Tracker (TCMT, [7]) strip detector have been operated with a common data acquisition providing the readout of ~ 18000 channels. AHCAL and TCMT share not only the same sampling material but also the same photo-detector readout via SiPM [8]. Other calorimeter designs for the ILC have been recently reviewed, e.g., in [9].

II ECAL Si-W prototype

A compact electromagnetic calorimeter requires that the absorber material should have a small Molière radius and a small radiation length (X_0). Tungsten is such a material, with a Molière radius of 9 mm and a radiation length of 3.5 mm. Furthermore, the ratio of interaction to radiation lengths is 27.4 so that hadronic showers typically develop later than electromagnetic showers. The choice of the pad size $1\times 1\text{ cm}^2$ for the physics prototype, is comparable to the Molière radius. The prototype has a total depth of 24 radiation lengths, achieved using 10 layers of $0.4 X_0$ (1.4 mm) thick tungsten absorber plates, followed by 10 layers of $0.8 X_0$ (2.8 mm) thick plates, and another 10 layers of $1.2 X_0$ (4.2 mm) thick plates, with an overall calorimeter thickness of 20 cm. This will ensure containment better than 98% for 50 GeV showers. A small tungsten thickness in the first layers ensures a good energy resolution at low energy. Each silicon layer has an active area of $18\times 18\text{ cm}^2$, segmented into modules of 6×6 readout pads of $1\times 1\text{ cm}^2$

each. The active area of the physics prototype hence consists of 30 layers of 3×3 modules, giving in total 9720 channels.

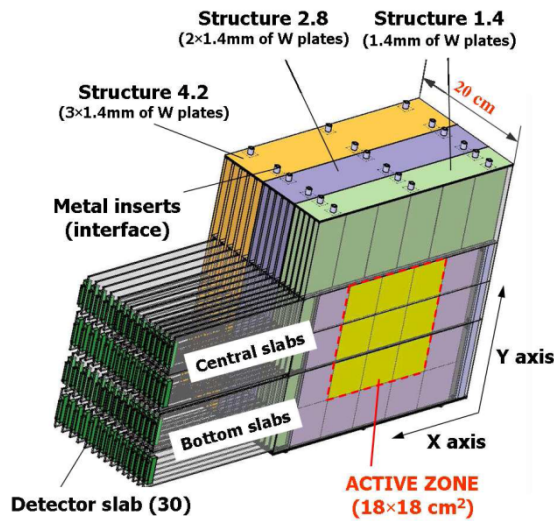


Figure 1 Schematic 3D view of the physics prototype.

Three independent structures can be distinguished, one for each thickness of tungsten (figure 1). Free space between two layers of tungsten is used for insertion of detection units, called detector slabs. One detector slab, shown in figure 2, consists of two active readout layers mounted on each side of an H-shaped supporting structure. The slab is shielded on both sides from the tungsten alveolar structure by an aluminium foil 0.1 mm thick, to protect the silicon

modules from electromagnetic noise and provide the wafer substrate ground. The H-shaped structure is 326 mm long and 125.6 mm wide. The active layer is made of a 14-layer printed circuit board, 2.1 mm thick and 600 mm long, holding high resistivity silicon wafers 525 mm thick. The wafers are cut into square modules of 62×62 mm², separated from each other by a 0.15 mm wide mounting gap. Two detector slabs are inserted per layer, into the central and bottom cells of the alveolar structure (see figure 1).

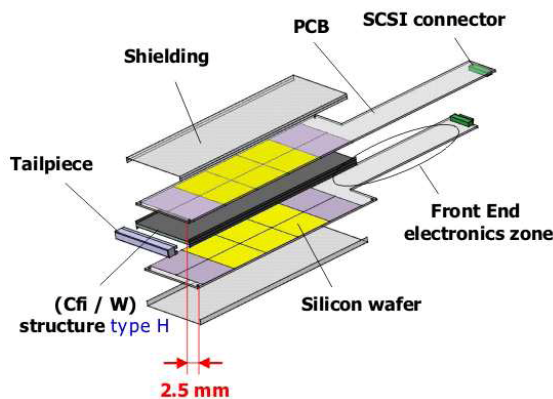


Figure 2 Schematic diagram showing the components of a detector slab.

The sensors are made from 4 inch diameter silicon wafers. A resistivity greater than 5 kΩ.cm is necessary to ensure a full depletion with a reasonable bias voltage, and to obtain low bulk leakage currents. A wafer thickness of 525 μm was chosen, to obtain a signal-to-noise ratio of about 10 at the end of the whole readout electronics chain. A minimum ionising particle

(MIP) produces about 80 electron hole pairs per mm of silicon, hence 42000 electrons are obtained for the 525 μm thickness, giving an allowable noise range for the readout electronics of up to 4000 electrons. Each wafer is used to make a module, consisting of a matrix of 6×6 PIN diodes (pads) of 1 cm². For the physics prototype, 270 modules are needed. The modules were produced by two manufacturers: the Institute of Nuclear Physics, Moscow State University, and ON Semiconductor Czech Republic in conjunction with the Institute of Physics, Academy of Sciences of the Czech Republic, Prague. The very-front-end (VFE) ASICs used to read out the silicon modules have been specifically designed for the prototype. The outputs of the VFE ASICs are off-line digitally converted by VME ADCs.

The calorimeter readout is based on the “Calice Readout Cards” (CRC) [10]. These are custom designed, 9U, VME boards derived from the Compact Muon Solenoid tracker front end

driver readout boards but with major modifications to the readout and digitisation sections. Each CRC is capable of reading out 1728 channels. The data volume per event from these channels is 4 kB. Six CRCs are required for the full ECAL readout of 9720 channels and these are housed in a single VME crate. The VME interface used is the SBS620 VMEbus-PCI bridge [11].

II.1 Beam tests

In August and October 2006, the ECAL was tested at CERN, in combination with the AHCAL prototype and the TCMT prototype, using electron and pion SPS-H6 beams. The 30 layers of the ECAL prototype were equipped with central slabs.

The energy of the electron/positron beams was varied from 6 to 50 GeV, to study linearity and resolution. The beam was positioned near the centre, edge and corner of the wafers to study the uniformity of the wafers and the impact of the passive areas. The ECAL prototype was rotated by 10° , 20° , 30° and 45° with respect to the beam direction to study the effects of angular incidence on the linearity and resolution. Finally, π^+ and π^- beams were taken with energies from 6 to 80 GeV. Over 22 million events were collected with electron beams and 25 million events with pion beams. In addition, more than 57 million muon events were collected for calibration purposes.

II.2 Calibration of ECAL

Muons are used to calibrate the detector in MIPs. After checking the stability in time of the noise, the conversion factor from ADC counts to MIP equivalent energies needs to be extracted per channel [12]. The event sample is selected by requiring the presence of a track which is consistent with being a MIP, based on two criteria. First, the total number of reconstructed hits in the 30 layers of the ECAL must be between 15 and 40. Then, the distance between two hits in consecutive layers must be less than 2 cm. As the residual pedestals are shown to be negligible compared to the estimated MIP signal (0.2% of a MIP), they are not subtracted from the measured value of the MIP peak position. With a mean noise of $12.9 \pm 0.1\%$ of a MIP, the noise tail is neglected and only the MIP contribution in the hit energy distribution is fitted.

For each channel, the distribution of hit energies (in ADC counts) is made from the sample of selected muons and fitted to a convolution of a Landau distribution and a Gaussian. The most probable value of the Landau function gives the calibration constant, while the standard deviation of the Gaussian gives an estimate of the noise value for each channel. For 6403 out of the 6480 channels of the prototype, the MIP calibration is obtained using the above procedure. For the remaining 77, special calibration procedures were developed.

II.3 Selection of electron events

The selection of single electron showers from data relies on the energy recorded in the ECAL. This energy, E_{raw} , is calculated with the three ECAL stacks weighted in proportion to the tungsten thickness:

$$E_{\text{raw}} = \sum_{i=0}^9 E_i + 2 \sum_{i=10}^{19} E_i + 3 \sum_{i=20}^{29} E_i$$

where E_i is the energy deposit in layer i . The distribution of E_{raw} is shown in figure 4 for a 20 GeV run. The electron peak around 5000 MIPs is clearly visible; however, the beam contamination with muons or pions gives an additional peak at 50 MIPs and the region between the two main peaks is populated with pions. Electron candidates are selected by requiring $125 < E_{\text{raw}}(\text{MIP})/E_{\text{beam}} < 375$ [12].

The significant pion contamination present in some of the runs is reduced by demanding a trigger signal from the threshold Čerenkov counter in the beam. The effect of this additional selection is indicated by the shaded region in figure 3.

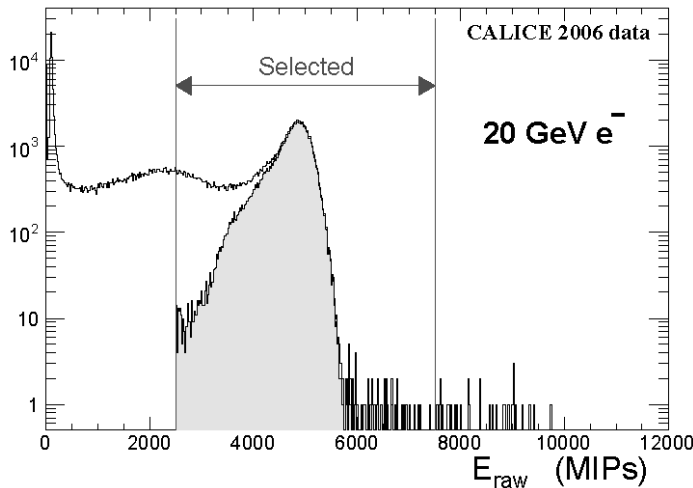


Figure 3 Distribution of total ECAL hit energies for a 20 GeV beam. The E_{raw} selection window and the shaded area obtained by demanding a signal from the Čerenkov counter are shown.

The inter-wafer gaps of 1.8 mm due to the guard rings have an influence on the response when showers traverse these regions of the calorimeter. In order to recover this loss and to have a more uniform calorimeter response, a simple method was investigated. The ECAL energy response, $f(x_b, y_b) = E_{\text{raw}}/E_{\text{beam}}$, is measured as a function of the shower

barycentre (x_b, y_b) using a combined sample of 10, 15 and 20 GeV electrons and the energy of each shower is corrected by $1/f$. The response function can be parameterised with Gaussian functions. To reduce the impact of the beam profile, only particles impinging in the middle of the wafers are selected. The fiducial volume in which the showers are fully contained in the ECAL was estimated from the radial shape of showers and leads to condition on the impact point of the track on the ECAL front face to be more than 4 cm from the ECAL borders.

II.4 Linearity and energy resolution

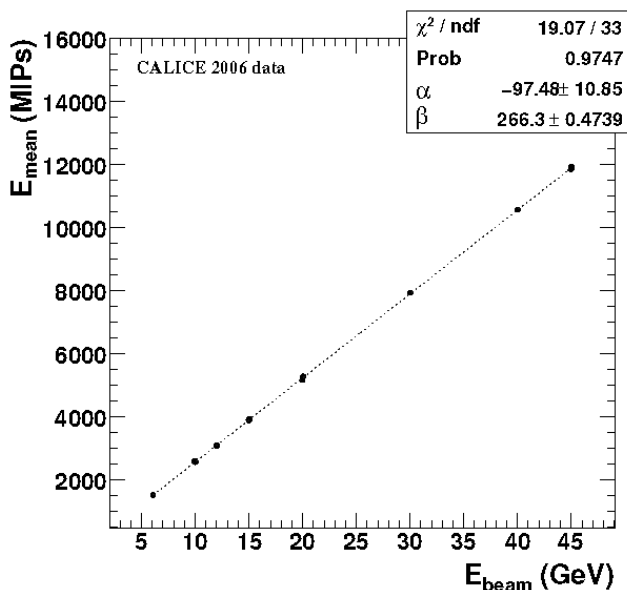


Figure 4 Linearity of the energy response of ECAL with respect to the beam energy.

The total response E_{rec} of the calorimeter is calculated as the weighted sum over energies deposited in 29 calorimeter layers. The weight takes into account the tungsten thickness as well as the contribution of the passive materials of the calorimeter: PCB, Al, glue, etc. A Gaussian fit is performed in the range $(-\sigma; +2\sigma)$ in order to extract the mean energy response and the dispersion. The sensitivity to the pion background and the influence of the

inter-wafer gaps are reduced by the asymmetry of the fit range. The linearity of the response with respect to the beam energy is described by $E_{\text{rec}} = \beta E_{\text{beam}} - \alpha$; where α and β are extracted from a fit to the data as shown in figure 4. The response of ECAL is linear at percent level as deduced from the residuals. The measured energy can be determined as $E_{\text{meas}} = (E_{\text{rec}} + \alpha)/\beta$. The relative energy resolution $\Delta E_{\text{meas}}/E_{\text{meas}}$ can be parameterised by a quadrature sum of stochastic and constant terms.

$$\frac{\Delta E_{\text{meas}}}{E_{\text{meas}}} = \frac{16.69 \pm 0.13}{\sqrt{E(\text{GeV})}} \oplus (1.09 \pm 0.06)\%$$

The value of the stochastic term is in agreement with expectations and will be compared with the simulation of the ECAL.

III Analog HCAL prototype

The AHCAL is a sampling calorimeter using standard steel as absorbers and scintillator tiles as the active medium. The millimetre size SiPM sensors are mounted on each tile and allow operation in high magnetic fields anticipated for the final detector. The scintillation light is collected from the tile via wavelength shifting fibres (WLS) embedded in a groove. This concept is different from existing tile calorimeters that have long fibre read-out and will allow to integrate both the photosensors and the front-end electronics into the detector volume.

Two main goals are envisaged by the physics prototype: to test the novel SiPM readout technology on a large scale and to accumulate data samples in beam tests to tune the particle flow algorithm and hadron shower models in GEANT4, respectively. The choice of dimensions of $1 \times 1 \times 1 \text{ m}^3$ was based on the requirement that the core of hadron showers with energies up to several tens of GeV is laterally fully contained. Existing reconstruction tools on detailed simulation studies of overlapping hadron showers in ILC events have shown that a transverse tile dimension of $3 \times 3 \text{ cm}^2$ provides an optimal two-particle separation and the anticipated jet energy resolution. The total thickness of the AHCAL prototype is 4.5 interaction lengths λ . In the test beam operation, the hadron calorimeter prototype is augmented with a tail catcher and muon tracker TCMT system [7], since high-energy hadrons leak out.

The AHCAL prototype consists of a sandwich structure of 38 absorber plates and 38 active layers containing in total 7608 scintillator tiles. Active layers up to layer 30 contain 216 scintillator tiles, while the last eight layers contain 141 scintillator tiles. All scintillator tiles in a layer are housed inside a rigid cassette called a module (see figure 5). A groove is milled into each scintillator tile into which a Kuraray Y11 wavelength-shifting fibre is inserted that collects the scintillation light. The fibre is coupled to the tile via an air gap to maintain the total reflection properties of the fibre.

A SiPM is a multipixel silicon photodiode operated in the Geiger mode [8]. The photosensitive area is $1.1 \times 1.1 \text{ mm}^2$ and contains 1156 pixels, each $32 \times 32 \text{ }\mu\text{m}^2$ in size. SiPMs are operated with a reverse bias voltage of $\sim 50 \text{ V}$, a few volts above the breakdown voltage. They have a gain $\sim 10^6$. The analog information is obtained by summing up the number of fired pixels that limits the dynamic range of SiPM. To break off the Geiger discharge a quenching resistor of a few M Ω is connected to each pixel and leads to pixel recovery time of up to 100 ns. More than 10000 SiPMs have been produced by the MEPHI/PULSAR group and have been tested at ITEP. The reverse bias voltage working point has been chosen such that a signal from a MIP, provided by the calibrated LED light, yields 15 pixels in order to ascertain a large dynamic range and to

have the MIP signal well-separated from the pedestal. The excellent resolution at low light intensity when only several pixels are fired provides self calibration and monitoring of each SiPM.

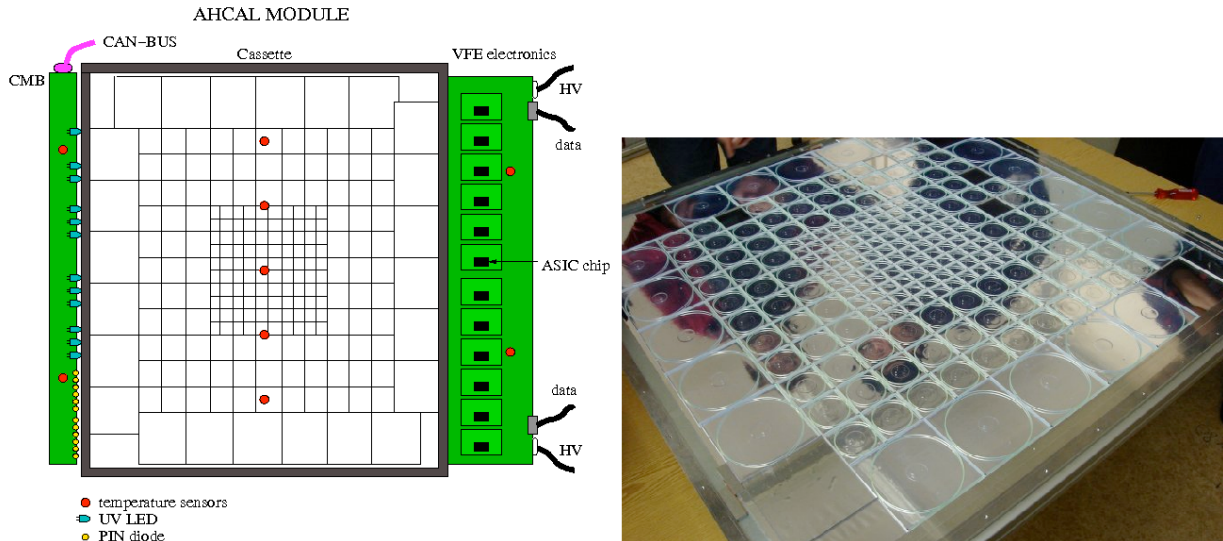


Figure 5 Schematic tile layout of a scintillator module for layers 1-30 (left). Photograph of tiles in a module (right).

We have built a monitoring system that distributes UV LED light to each tile via clear fibre. The monitoring system performs three different tasks. First, at low light intensity provides a calibration of the ADC in terms of pixels. Second, monitors all SiPMs during test beam operations with a fixed-intensity light pulse. Third, measures the full SiPM response function by varying the light intensity from zero to the saturation level. By varying the voltage the LED intensity can cover the entire dynamic range of all SiPMs [13]. In addition, we use high precision power supplies for the SiPM bias voltage. The thermo-couples placed in each cassette are read out regularly by a slow control system and the temperature is recorded in a data base for later off-line correction.

The front-end electronics is matched to the SiPM needs. A single ASIC houses an 18-fold multiplexed chain of preamplifier, shaper, and sample-and-hold. The signals from 12 ASICs are fed into one of the eight input ports of the CALICE readout card and are digitized by 16-bit ADCs. The AHCAL and the ECAL readout concept are based upon the same architecture described in the Chapter II as well as the same DAQ system.

III.1 Beam tests

The AHCAL was installed together with ECAL and TCMT in the CERN SPS-H6 beam line in September 2006 with 23 active layers only. To cover a sufficient fraction of the longitudinal shower development, it was decided to use two different samplings. The first seventeen layers, in which $\sim 75\%$ of the shower energy is deposited, were fully equipped. The following thirteen layers were equipped with the remaining 6 modules, one every other layer. This configuration covers the part with the statistically highest activity whilst still giving a $\sim 3.5 \lambda$ deep calorimeter.

Full commissioning of 38 active layers was achieved for CERN runs in 2007 covering the total depth of 4.5λ .

III.2 Muon and electron analysis

The validation of the calibration procedure and the MC digitization is obtained by the study of the calorimeter response to muons and electromagnetic showers. The three calorimeters (ECAL, AHCAL and TCMT), as well as the full instrumentation of the SPS-H6 beam line at CERN, have been implemented in MOKKA [14]. The true GEANT4 response of the detectors is digitized to include the SiPM response function, Poisson smearing, noise and optical cross-talk between adjacent scintillator tiles. In order to validate the digitization steps, data is compared to MC for well understood physics processes sensitive to the calibration procedure steps. All calorimeter cells are equalized using the signal from a MIP. The response of the whole calorimeter and of the single cells to a MIP is investigated.

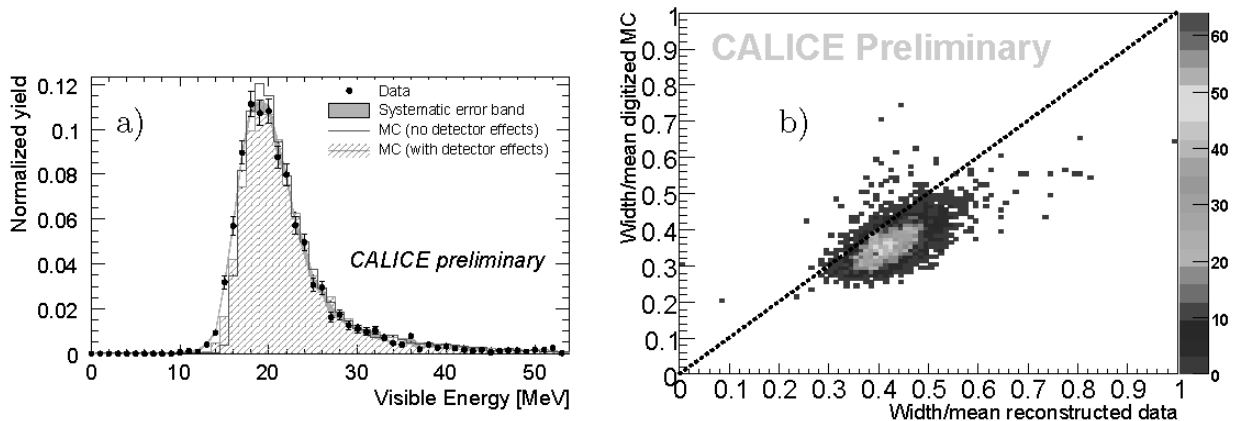


Figure 6 a) Total visible energy deposited by a 120 GeV muon in the AHCAL (points), compared to true and digitized MC. b) Cell-by-cell correlation of the MIP resolution between data and digitized MC.

The energy deposited by a muon traversing 23 layers of the AHCAL is shown in figure 6a. The distribution is compared to simulation both with and without digitization. In both cases the MC well reproduced the mean value and the spread of the distribution. Figure 6b shows cell-by-cell the MIP resolution correlation between data and digitized MC. The MIP width is influenced by Poisson smearing and noise. The correlation is good, but the MC width is about 10% smaller than for the data. This effect may be related to the tile non-uniformity, which is not yet included in the digitization [15].

The response to positrons is reconstructed as the energy sum of all hits above threshold cut of 0.5 MIP over the whole detector in the range of 10-50 GeV. It is linear within errors up to 30 GeV beam momentum. A significant remaining non-linearity of about 4% is observed for 50 GeV positrons. The energy resolution for positrons is evaluated for data and digitized MC and presented in figure 7. A sum in quadrature of noise ($1/E$), stochastic ($1/\sqrt{E}$) and constant terms is used to fit the points. The noise term is fixed from random trigger events to 2 MIP. The stochastic terms in data and MC are $(22.6 \pm 0.1_{\text{fit}} \pm 0.4_{\text{calib}})\%/\sqrt{E}$ and $(20.9 \pm 0.3_{\text{fit}})\%/\sqrt{E}$, respectively. Both constant terms for data and MC are consistent with zero within errors.

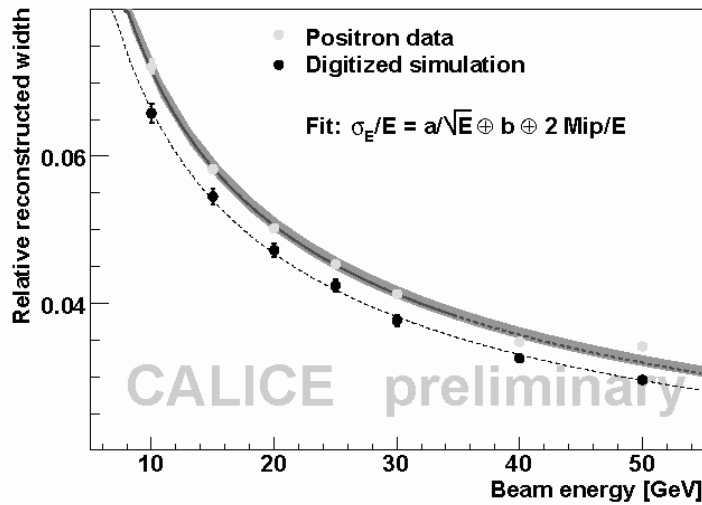


Figure 7 Relative width of the reconstructed energy as a function of beam energy. The fit results (excluding points at 40 and 50 GeV) for data show in the gray band the effect of the calibration uncertainty on the saturation scale. The lower broken curve and full circles are for the MC.

III.3 Pion analysis

The results are based on pion runs from 2006 at beam energies from 6 to 80 GeV. The range 6-20 GeV is a negative pion sample; the range 30-80 GeV is a positive pion sample. Calibrated pion events which interact in the ECAL as MIP-like particles are selected, which have no energy leaking to the TCMT. Additionally a loose cut on the number of hit in the AHCAL is made ($N_{\text{hits}} > 8$) to exclude nearly empty events in the AHCAL. Then a track finder is applied.

The total energy of a pion shower is obtained as the sum of energy deposited in all free calorimeters multiplied by the appropriate sampling factor. Only cells with energy above a threshold of 0.4 MIP are considered. At each energy, the distribution is fit with a Gaussian function in a range of $\pm 2\sigma$. The response and resolution are the mean and sigma values from the fit. The calorimeter response as a function of energy is shown in figure 8. At most a 2.5% negative deviation from linearity is observed at 80 GeV.

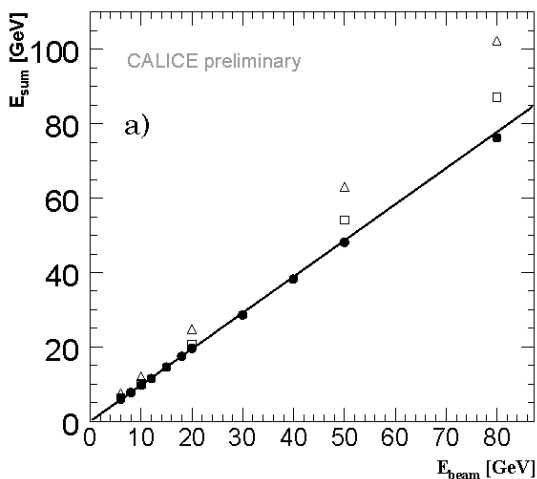


Figure 8 Linearity of the AHCAL and TCMT combined response to pions. Black circles are data, open squares digitized LHEP and open triangles are digitized QGSP_BERT – two hadronization models used in the simulation.

Test beam data were taken with single pions. These events can be overlaid offline for the study of showers separation in the calorimeter. These fully contained showers in the AHCAL are selected according to their relative distance and overlaid on a cell basis. The energy of the overlaid event in each cell is

the sum of the single pion energies. The overlaid events are then input to a clustering algorithm which identifies the two clusters and measures their total energy. A track-wise clustering algorithm is used, which is an algorithm developed for particle flow in the full ILC detector [16]. Then one of the two pions is considered to be a charged hadron and its energy measured in the calorimeter is replaced by the known beam energy. From the two tracks visible as MIPs in the ECAL, the one is assigned to the cluster with cluster position (projection of the centre of gravity to the x,y plane) closest to the track.

To quantify the result of the particle flow approach compared to the ideal particle flow, the efficiency of shower separation has been defined. For events where exactly two clusters have been found, the cluster energy E_{cluster} in an interval of $\pm 3\sigma$ of E_{calo} is integrated and compared to E_{calo} . The ratio of these two quantities defines the particle flow efficiency,

$$eff_{\text{Pflow}} = \frac{\int_{-3\sigma}^{+3\sigma} E_{\text{cluster}}}{\int_{-\infty}^{+\infty} E_{\text{calo}}}$$

The ideal particle flow case corresponds to infinitely separated clusters for which $E_{\text{cluster}} = E_{\text{calo}}$. Figure 9 shows the efficiency of particle flow for 6-20 GeV charged particle (track) separated from the 20 GeV neutral cluster. The efficiency increases for larger distances between particles and for lower energy of the neutral particle.

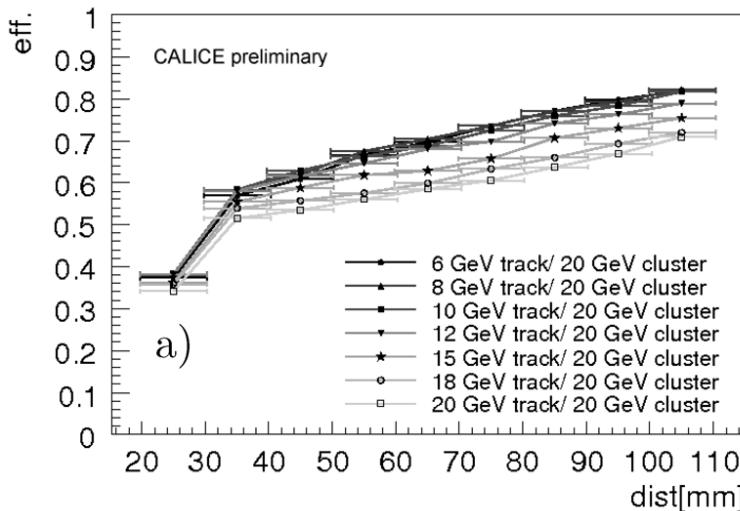


Figure 9 Efficiency of the particle flow as a function of particles separation for a 20 GeV cluster.

IV Conclusions

The physics prototypes of electromagnetic and hadron calorimeters have been built in the CALICE Collaboration and were tested in the CERN beams. The response of Si-W ECAL was measured for energies 6-45 GeV. The calorimeter is linear to 1% level. The energy resolution has a stochastic term of $16.69 \pm 0.13\%$ and constant term 1.09 ± 0.06 (statistical). The scintillator-steel HCAL has been tested on electromagnetic data. The calorimeter is linear up to 30 GeV, a deviation of 4% is visible for 50 GeV positrons, which requires more detailed studies. The comparison to hadron data shows linearity up to 80 GeV at the 2.5% level. The first application of a particle flow reconstruction algorithm has been applied on the pion data in the energy range 6-20 GeV and represent an important step in the verification of the algorithm on the real data.

Acknowledgement

The author would like to thank to all colleagues from the CALICE collaboration for the excellent work done to bring the calorimeters into operation and the analysis of the test beam data. Thanks especially go to D. Bailey, D. Boumediene, C. Carlogănu, G. Eigen, E. Garutti, A.-I. Lucaci-Timoce, B. Lutz, I. Polák, F. Sefkow, V. Vrba. This work was supported in part by the Ministry of Education of the Czech Republic under the projects LC527 and INGO-1P05LA259.

References

- [1] The CALICE collaboration, <http://polywww.in2p3.fr/activities/physique/flc/calice.html> .
- [2] Behnke T et al., *Reference Design Report "Volume 4: Detectors"*, (2008), available at <http://lcdev.kek.jp/RDR>.
- [3] Thomson M.A., In *Proceedings of 2007 International Linear Collider Workshop (LCWS07), Hamburg, Germany, 2007*.
- [4] Brau J.E. et al., In *Proceedings of 1996 DPF/DPB Summer Study on New Directions in High Energy Physics, Snowmass, CO, 1996 econf C960625 (1996) DET077*.
- [5] Repond J. et al., *JINST* **3** (2008), P08001-P08033.
- [6] Eigen G., "The Calice scintillator HCAL testbeam prototype", In *Proceedings of XII International Conference on Calorimetry in High Energy Physics, Chicago, IL, 2006*, 49n-58n.
- [7] Chakraborty D., In *Proceedings of 2005 International Linear Collider Workshop (LCWS05), Stanford, CA, 2005*.
- [8] Buzhan P., Dolgoshein B., Filatov L., Ilyin A., Kantzerov V., Kaplin V., Karakash A., Kayumov F., Klemin S., Popova E., Smirnov S., *Nucl. Instrum. Meth. A* **504** (2003), 48.
- [9] Cvach J., *IEEE Trans. Nucl. Sci.*, **50** (2008), 1308-1313.
- [10] Warren, A. "A VME readout system for the CALICE electromagnetic calorimeter", presented at IEEE Nucl. Symp., Rome, Italy, October 2004.
- [11] SBS620 VMEbus-PCI bridge, <http://www.gefanuembedded.com>.
- [12] Boumediene D., "Response of the CALICE Si-W ECAL physics prototype to electrons", will be published in *Proceedings of XIII International Conference on Calorimetry in High Energy Physics (Calor08), Pavia, Italy, 2008*.

- [13] Polák I, “*Development of Calibration system for AHCAL*”, presented at ECFA&GDE meeting, Valencia, Spain, November 2006, http://www-hep2.fzu.cz/calice//files/ECFA_Valencia.Ivo_CMB_Devel_nov06.pdf
- [14] “*MOKKA – a detailed GEANT4 simulation for the International Linear Collider detectors*”, <http://polywww.in2p3.fr/activities/physique/geant4/tesla/mokka/mokka.html>.
- [15] Garutti E., “*CALICE scintillator HCAL – electromagnetic and hadronic shower analysis*”, will be published in *Proceedings of XIII International Conference on Calorimetry in High Energy Physics (Calor08), Pavia, Italy, 2008*.
- [16] Morgunov V., Raspereza, “*Novel 3D clustering algorithm and two particle separation with tile HCAL*”, ILC note: LC-TOOL-2004-022, <http://www-flc.desy.de/lcnotes/>.